Mono- and di-substituted pyrene-based donor-π-acceptor systems with phenyl and thienyl π-conjugating bridges

Monica Irina Nan, Eszter Lakatos, Gavril-Ionel Giurgi, Lorant Szolga, Riccardo Po, Anamaria Terec, Siriporn Jungsuttiwong, Ion Grosu, Jean Roncali

Mono- and di-substituted pyrene-based donor-π-acceptor systems with phenyl and thienyl π-conjugating bridges

Monica Irina Nan,[a1] Eszter Lakatos,[a1] Gavril-Ionel Giurgi,[a,b] Lorant Szolga,[a,b] Riccardo Po,[c] Anamaria Terec,[a] Siriporn Jungsuttiwong,[d] Ion Grosu*[a] and Jean Roncali*[a,e]

[a]Babes-Bolyai University, Faculty of Chemistry and Chemical Engineering, Department of Chemistry and SOOMCC, Cluj-Napoca, 11 Arany Janos str., 400028, Cluj-Napoca, Romania
[b]Optoelectronics Group, Base of Electronics Department, ETTI, Technical University of Cluj-Napoca, Str.Memorandumului, Nr.28, Cluj-Napoca, 400114, Romania
[c]Research Center for Renewable Energies and Environment, Instituto Donegani, Eni S. p. A., via Fauser 4, IT-28100 Novara, Italy
[d]Center for Organic Electronics and Alternative Energies, Department of Chemistry University of Ubon Ratchathani 34190, Thailand
[e]Moltech Anjou CNRS, University of Angers, 2 Bd Lavoisier, 49045, Angers, France

[1]:these two authors contributed equally to the work

Keywords. Pyrene, donor-acceptor, pi-conjugated systems, internal charge-transfer

Abstract

The synthesis of a series of four donor-π-acceptor (D-π-A) compounds involving pyrene derivatized with hexylcyanoacetate acceptor groups connected by phenyl or thienyl π-conjugating spacers is described. The electronic properties are characterized by UV-Vis absorption spectroscopy, cyclic voltammetry theoretical calculations and solvatochromism experiments. The results indicate that the thienyl connectors leads to D-π-A systems with smaller optical gaps and stronger internal charge transfers attributed to the combined effects of the lower resonance energy of thiophene, the smaller twist angles between the pyrene block and the π-connector and the deformability of the thiophene ring.

1. Introduction

Pyrene is the smallest peri-fused polycyclic aromatic hydrocarbon widely investigated for its interesting combination of electronic and structuring properties [1]. Owing to its planar geometry and rigid structure, pyrene possess a strong propensity to π-stacking, a property which is widely used to attach a large variety of functional groups onto graphite-like structures such as

fullerenes [2,3], carbon nanotubes [4,5] or graphene [6]. Pyrene has also been used to control the molecular packing of organic semiconductors based on π-conjugated systems in order to improve their charge-transport properties [7-9]. The high electron density and photoluminescence properties of pyrene have been exploited for the development of emitters for light-emitting diodes (OLEDs) [10-13]. On the other hand, pyrene has also been used a building block for the synthesis of chromophores for dye-sensitized solar cells (DSSCs) [14] and organic photovoltaics cells (OPV) [15-17]. These various applications have given rise to the development of a rich synthetic chemistry aiming at the control of the electronic properties of pyrene-based systems in order to modulate the energy levels of their frontier orbitals and their energy gap as well as their intermolecular interactions. The modulation of the electronic properties of pyrene can be achieved by different strategies involving the introduction of electron-donor and/or electron acceptor groups [1, 7-17] eventually combined with the extension of the π-conjugated system by grafting or aromatic moieties or by annulation [18]. For OPV applications, pyrene has been essentially involved in the synthesis of electron donor materials [14-17] however, recent work has reported examples of non-fullerene acceptor materials based on a pyrene core [19]. Recently, Gao and coworkers have described potential n-type organic semi-conductors based on mono and disubstituted pyrenes derivatives in which electron acceptor dicyanovinyl groups are connected to the pyrene block by 3-dodecyl-thienyl spacers [20]. The alkyl chains were introduced on the thiophene ring to ensure the solubility of the compounds.

As a first step in the exploration of structure properties relationships in pyrene derivatives designed as potential donor building blocks for single-material organic cells (SMOSCs) [21,22], we report herein on the synthesis and electronic properties of two series of mono-and di-substituted pyrenes in which cyanoester electron acceptor groups are connected to the pyrene core *via* phenyl and thienyl π-conjugating bridges (**1-4,** Scheme 1). Unlike the already reported compounds [20], the solubility of these new molecules is ensured by the hexyl chains of the cyanoester in order to limit steric hindrance between the thiophene rings and the peripheral hydrogen atoms of pyrene. After screening of their electronic properties, these systems are intended to be connected to non fullerene electron acceptors (NFA) by means of an hydroxyl group which will be fixed at the end of the cyanoalkyl chain according to an already reported approach [23]. Since highly efficient NFA absorb in the red or NIR part of the solar spectrum, they are generally associated with donor blocks absorbing at shorter wavelengths [22,24]. In fact,

the situation is inverted compared to SMOSCs involving fullerenes acceptors for which donors with red-shifted absorption are needed [21,22]. The synthesis of the new compounds is described and structure-properties relationships are discussed on the basis of the results of UV-Vis absorption spectroscopy, cyclic voltammetry, theoretical calculations and solvatochromism experiments.

2. Results and discussion

The synthesis of the target compounds is depicted in **Scheme 1**. Mono-aldehydes **5** and **7**, dialdehyde **6** and dithienyl-pyrene **8** where synthesized according to literature procedures [25-30]. Vilsmeier-Haack di-formylation of the dithienyl pyrene **8** afforded dialdehyde **9** in 96 % yield. Knoevenagel condensation of aldehydes **5-7** and **9** with hexyl cyanoacetate led to the target compounds **1-4** in 30 to 70 % yields. The structure and purity of all target compounds were determined by ^{1}H and ^{13}C NMR and HRMS spectrometries giving satisfactory results.

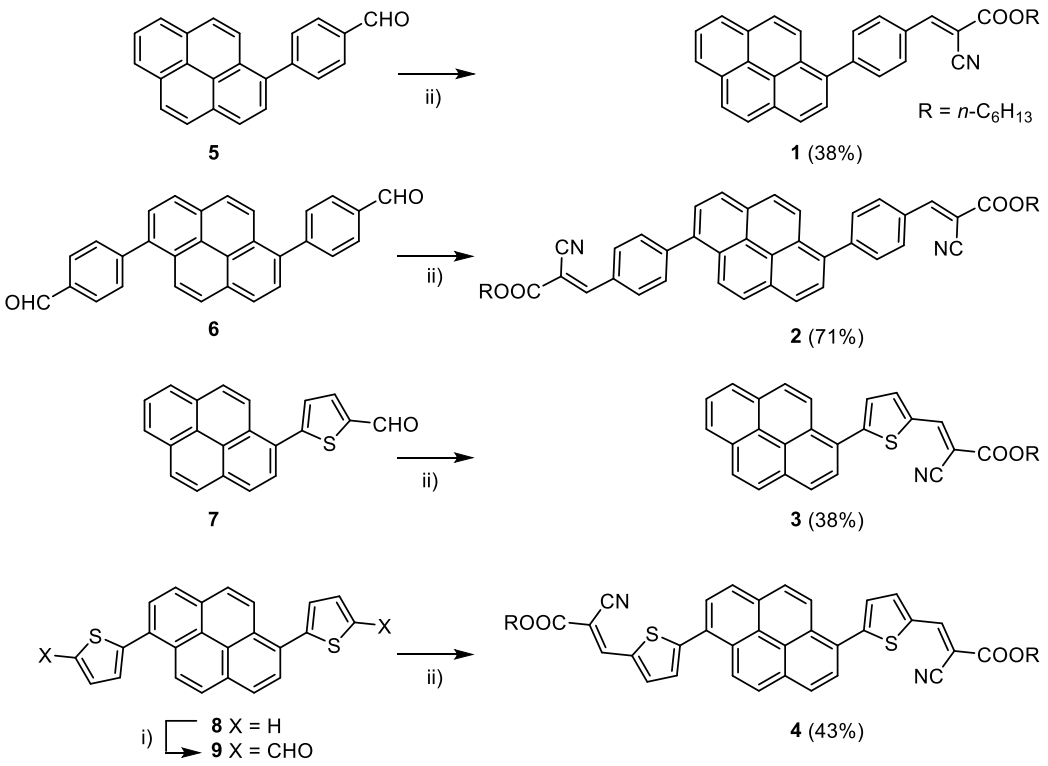

Scheme 1. Synthesis of the target compounds **1-4**. i) $POCl_3$, DMF, dichloroethane ii) *n*-hexyl-cyanoacetate, Et_3N, $CHCl_3$, rflx.

Fig. 1. shows the UV-Vis absorption spectra of the compounds in DCM solutions while the corresponding data are listed in Table 1. The spectrum of all compounds shows a first band in the 300-350 nm region assigned to the π–π* transition of the pyrene block followed by a broader band in the 400-500 nm range corresponding to an internal charge transfer (ICT). The spectra of the phenyl substituted compounds **1** and **2** show that the introduction of a second cyanoester acceptor unit on the pyrene block produces a bathochromic shift of the absorption maximum of both transitions together with an increase from 0.64 to 0.78 of the relative intensity of the ICT band *vs* the π–π* transition.

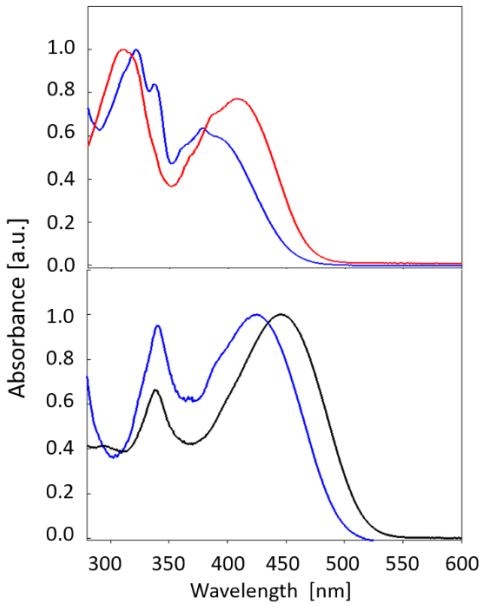

Fig. 1. UV-Vis absorption spectra of the target compounds in DCM. Top phenyl compounds blue**:** mono-substituted **1**, red : disubstituted **2**, bottom thienyl compounds blue: mono-substituted **3**, red: disubstituted **4**.

This result is consistent with an increase of the strength of the ICT. Both spectra exhibit a discernible vibrational fine structure which is absent in the spectra of the thienyl compounds **3-4**. This difference suggests a more rigid structure for the phenyl substituted compounds. Comparison of the data for compounds **1** and **2** to those of their thienyl analogs **3** and **4** shows that the replacement of the phenyl by the thienyl π-spacer produces a 47 nm bathochromic shift of the maximum of the ICT band for the mono-substituted compounds **3** *vs* **1** and 32 nm for the disubstituted compounds **4** *vs* **2**. Comparison of the relative intensity of the ICT *vs* π–π* bands for compounds **1**, **3** and **2**, **4** reveals an inversion of the ratio for the thienyl compounds. Taking

this ratio as an indication of the strength of the ICT [28], suggests a stronger ICT for the thienyl compounds, consistent with a better conjugating effect of thiophene *vs* benzene [29].

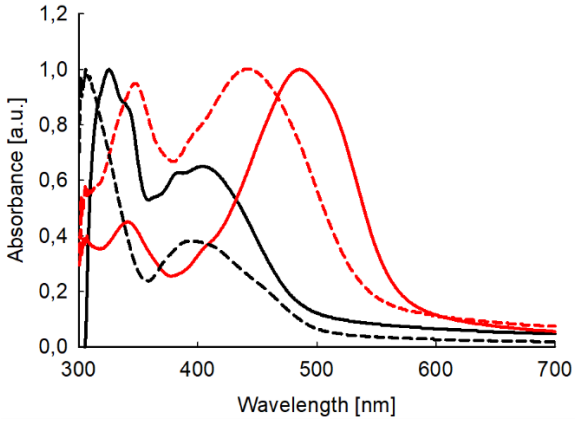

Fig. 2. UV-Vis absorption spectra of thin films spun-cast on glass. Black: phenyl compounds, dashed line: **1**, solid line: **2.** Red: thienyl compounds, dashed line: **3**, solid line: **4**.

Fig. 2 shows the UV-Vis absorption spectra of thin films of compounds **1**, **2**, **3** and **5** deposited on glass by spin-casting of chloroform solutions. Comparison with the data recorded in solution (Table 1) shows that the absorption maximum of the ICT band in the films spectra presents a 12 nm bathochromic shift for compound **1** and no shift for compound **2**. In contrast, the spectra of films of the thienyl compounds reveal a 16 nm red shift of λ_{max} for compound **3** and 40 nm for compound **4**. These drastically different behaviors suggest that for the thienyl compounds, the passage from the solution to the solid state results in a planarization of the conjugated structure, possibly assisted by the deformability of the thiophene ring [30]. The band gap of the materials estimated from the absorption onset of the films show that as expected, the thienyl compounds present significant smaller values than their phenyl counterparts (Table 1).

Table 1. Results of UV-Vis absorption spectroscopy for compounds **1-4** in DCM solution and as thin films on glass and cyclic voltammetry data recorded in 0.10 MBu_4NPF_6/DCM.

Compd	$\lambda_{max\ (soln)}$ [nm]	$\lambda_{max\ (film)}$ [nm]	ICT/ππ*	E_{pa} [V]	E_{pc} [V]	E_g [eV]
1	308, 377	385	0.64	1.33	-1.35	2.48
2	336, 405	404	0.78	1.35	-1.30	2.40

3	340, 424	440	1.02	1.32	-1.30	2.20
4	340, 445	485	1.47	1.34	-1.23	2.15

The cyclic voltammograms (CV) of compounds **1-4** have been recorded in DCM in the presence of tetrabutylammonium hexafluorophosphate as the supporting electrolyte (Fig. 3). All compounds present very similar CVs with an anodic peak potential (E_{pa}) at *ca* 1.30 V. The reversibility of the oxidation process indicates the formation of a stable cation radical. This reversibility which contrasts with the irreversible CVs of the parent compounds containing 3-substituted thiophenes, [20] suggests a better effective conjugation associated with the reduction of steric interactions.

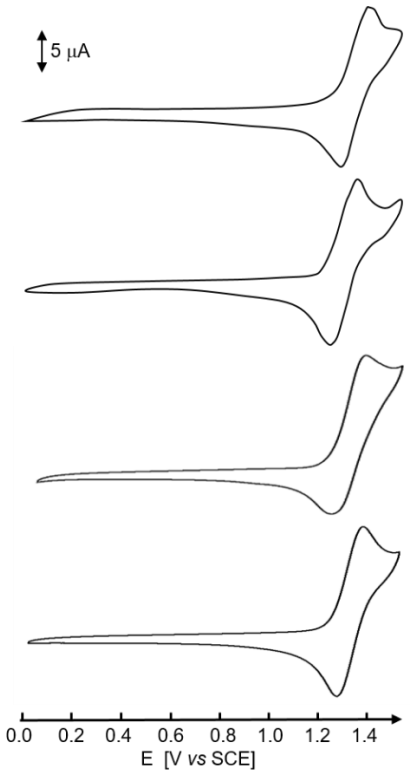

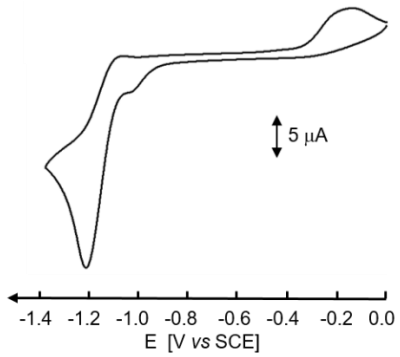

Fig. 3. Oxidation CVs for compounds **1-4** (top) and reduction CV of compound **4** (bottom) in 0.10 M Bu_4NPF_6/DCM, Pt electrodes, Ref. SCE, scan rate 100 mV s^{-1}.

The CVs recorded in the negative potential region exhibit an irreversible reduction wave peaking around E_{pc}= -1.30 V as exemplified for compound **4**. The small anodic wave observed on the reverse scan can be attributed to the re-oxidation of some products of degradation of the irreversible reduction. This marked difference between a reversible oxidation leading to stable cation radicals and the irreversibility of the reduction process suggests that these compounds could be more suitable as p-type organic semiconductors rather than as n-type, as recently proposed [20]. Compounds **1** and **2** with phenyl connecting groups present slightly more positive E_{pa} value than their thienyl counterparts. On the other hand, a small positive shift of the reduction wave is observed for the di-substituted compounds, as expected from the introduction of a second electron withdrawing cyanoester group. These results show that the type of connecting group and the number and position of the cyanoester electron withdrawing groups have little influence on the oxidation and reduction potentials of the system which is surprising in view of the smaller HOMO-LUMO gap of the thienyl compounds indicated by optical data. While we have no definitive explanation, this apparent discrepancy might be related to geometrical changes of the molecules in their excited state.

In order to complete these results, quantum chemical calculations based on density functional methods have been performed with the Gaussian 09 package. Becke's three-parameter gradient corrected functional (B3LYP) with 6-31G(d,p) basis was used to optimize the geometry and to compute the electronic structure. The optimized structures of the four molecules (Fig. 4) show that in each case the phenyl or thienyl ring form a large dihedral angles with the pyrene core. The calculated values of these dihedral angles and the energy levels of the frontier orbitals are gathered in Table 2. The results show that dihedral angles (θ) of *ca* 55 ° are found for compounds **1** and **2** whereas the thienyl compounds present *ca* 5° smaller dihedral angle

indicating a slightly reduced steric hindrance to planarity and hence a better effective conjugation. The data in Table 2 predict a moderate decrease of both the HOMO and LUMO levels for the disubstituted compounds in qualitative agreement with the CV data.

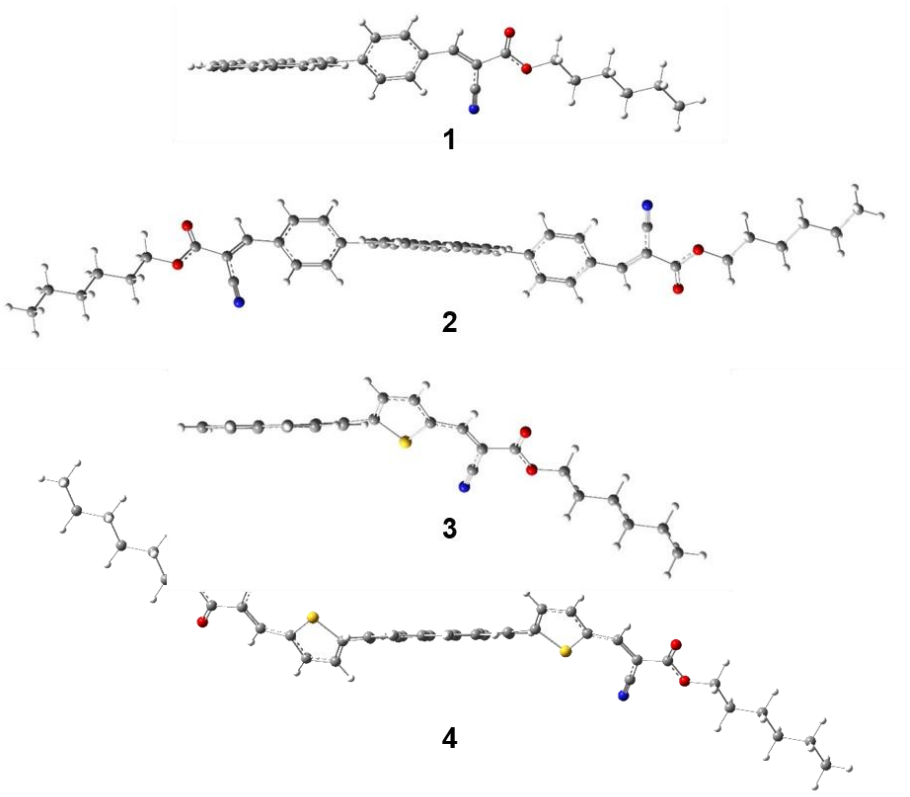

Fig. 4. Optimized geometries of compounds **1-4**

Table 2. Calculated energy levels of the HOMO and LUMO for compounds **1-4** and values of the dihedral angle between the pyrene and the phenyl or thienyl ring

.

Compd	E_{HOMO} [eV]	E_{LUMO} [eV]	ΔE [eV]	θ [°]
1	-5.72	-2.71	3.01	55
2	-5.82	-2.86	2.95	56
3	-5.73	-2.78	2.95	47
4	-5.83	-2.99	2.99	49

The distribution of the HOMO and LUMO coefficients represented in Fig. 5 shows that for all compounds, the HOMO is essentially distributed over pyrene block, while the highest LUMO coefficients are observed on the cyanoester substituted phenyl or thienyl ring.

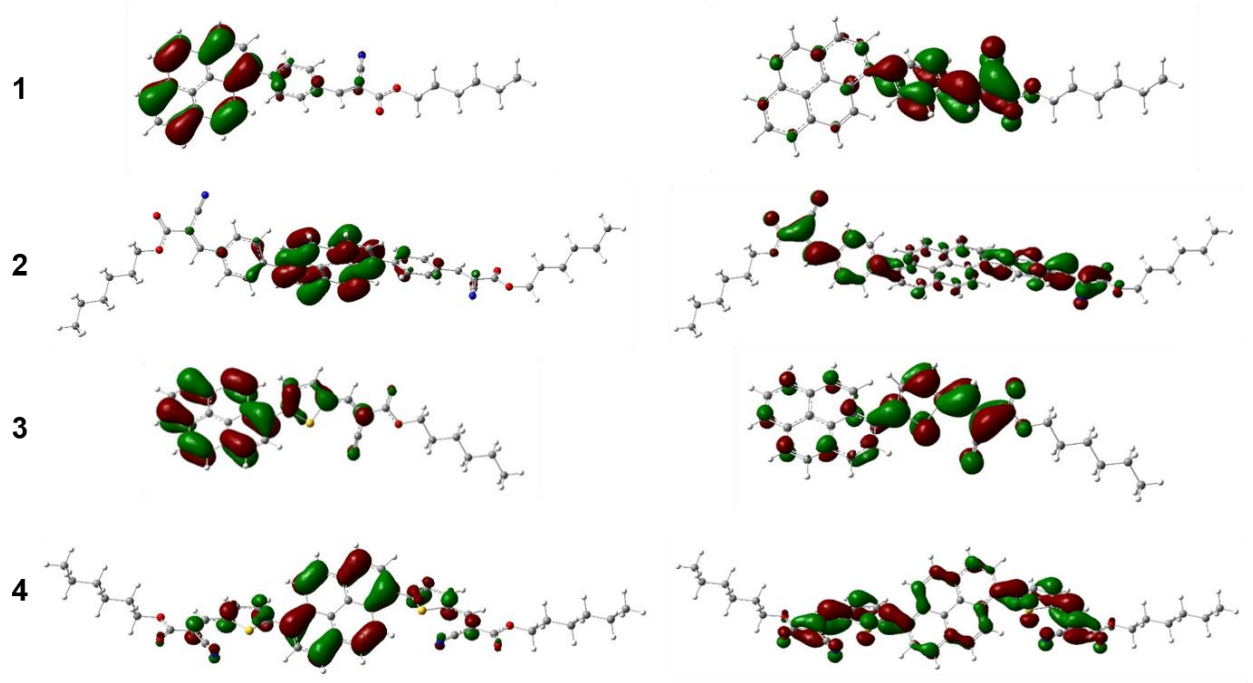

Figure 5. distribution of the HOMO and LUMO for compounds **1-4**.

The absorption and fluorescence emission spectra of the molecules have been analyzed in solvents of increasing polarity. A cursory evaluation of the fluorescence efficiency in THF relatively to diphenyl anthracene shows that all compounds present very low values, in the range of 2-5%, in agreement with recent results on related compounds [20]. Table 3 lists the position of absorption and emission maxima of compounds **1-4** in toluene, THF, DCM and acetone. These data show that the solvent polarity has only a minor effect on the absorption maximum of the molecules. In contrast, the increase of the solvent polarity produces a large bathochromic shift of the emission maximum resulting in large increase of the Stokes shift between absorption and emission. Thus, for compounds **1** the emission maximum (λ_{em}) undergoes a 70 nm red shift between toluene and acetone while the Stokes shift between the absorption and emission maxima increases by 2830 cm^{-1}. These results suggest a large increase of the dipole moment of the molecule between the ground and the excited state; the rearrangement of the solvent around the

molecule leading to a decrease of the energy of the excited state. The results for compound **2** reveal a similar red shift of λ_{em} between toluene and acetone (71 nm) but for each solvent, the Stokes shift is smaller than for compound **1** suggesting a smaller increase of the dipole moment in the excited state. This result reflects a partial annihilation of the dipole moment of the molecule due to the opposite directions of the vectors of dipole moments of the two A-π-D systems. A similar behavior is observed for the mono and disubstituted thienyl compounds **3** and **4** with a smaller Stokes shift for the di-substituted compound **4** in every solvent. However, a major difference with phenyl compounds is the considerably smaller red shift observed between the λ_{em} in toluene and acetone, *ca* 20 nm instead of 70 nm for **1** and **2**. A possible interpretation for these different behaviors could be related to a smaller increase of the dipole moment of the thienyl compounds in the excited state due to the fact that these compounds already possess larger dipole moments in the ground state, an hypothesis consistent with the much larger ICT of these compounds however, further experimental and theoretical work is needed to clarify this point.

3. Conclusion

Four D-π-A compounds involving electron-acceptor cyanovinyl ester groups connected to a pyrene core by phenyl and thienyl conjugating bridges have been synthesized. Cyclic voltammetric results show that all compounds are reversibly oxidized into stable cation radicals but irreversibly reduced. UV-Vis absorption data show that the thienyl compounds exhibit significantly smaller band gaps and stronger internal charge transfer probably due to the synergistic effect of the lower resonance energy of thiophene *vs* benzene and of the larger plasticity of the thiophene ring. In the solid state all compounds absorb in the 400-600 nm spectral range and are thus well suited for an association with non-fullerene acceptors in single material organic solar cells.

Table 3. Absorption and fluorescence emission maxima of compounds **1-4** in solvents of increasing polarity

Compd.	Solvent	λ_{abs} [nm]	λ_{em} [nm]	λ_{em} [cm^{-1}]	*SS* [cm^{-1}]
1	Toluene	378	490	20408	6050
	THF	377	540	18518	8010

	DCM	377	557	17953	8580
	Acetone	374	560	17857	8880
2	Toluene	408	491	20366	4140
	THF	405	544	18382	6310
	DCM	412	555	18018	6250
	Acetone	385	562	17793	8180
3	Toluene	425	536	18656	4870
	THF	418	548	18248	5670
	DCM	424	554	18050	5530
	Acetone	410	559	17889	6500
4	Toluene	443	545	18348	4220
	THF	439	556	17985	4790
	DCM	445	555	18018	4450
	Acetone	431	563	17761	5440

Experimental

Reagents and chemicals from commercial sources were used without further purification. Reactions were carried out under argon atmosphere unless otherwise stated. Solvents were dried and purified using standard techniques. Thin layer chromatography was performed on Silica gel 60 chromatography plates F254. Column chromatography was performed with analytical-grade solvents using silica gel (technical grade, pore size 60 A). Compounds were detected by UV irradiation or staining with 2,4-dinitrophenylhydrazine or $KMnO_4$ solutions, unless stated otherwise. NMR spectra were recorded with a Bruker AVANCE III 600 (1H, 600 MHz and 13C, 150 MHz). Chemical shifts are given in ppm relative to TMS and coupling constants J in Hz. HR-MS spectra in APCI and ESI mode ionization were recorded with an LTQ XL Orbitrap ThermoScientific mass spectrometer. UV-Vis measurements were performed in dichloromethane (DCM) (HPLC) at room temperature using a Cecil Super Aquarius spectrophotometer. Cyclic voltammetry was performed in DCM (HPLC grade). Tetrabutylammonium hexafluorophosphate, Aldrich was used without purification. Solutions were deaerated by argon bubbling prior to each experiment. Experiments were carried out in a one-compartment cell equipped with platinum

electrodes and saturated calomel reference electrode (SCE) with a Biologic SP-150 potentiostat with positive feedback compensation.

5,5'-(pyrene-1,6-diyl)bis(thiophene-2-carbaldehyde) (**9**).

DMF (26 mmol) was added to a solution of **9** or **11** (1 mmol) in 1,2-dichloroethane (32 mL). $POCl_3$ (20 mmol) was slowly added at 0°C. The mixture was stirred at 85°C for 24 h, then treated with ice water (200 mL) for 0.5 h and extracted with DCM. The organic phase was washed with brine and water and dried ($MgSO_4$). After solvent removal, the residue was chromatographed. Eluent 3:5 Petroleum ether (PE)/DCM. Yield 145 mg (93%). Yellow-orange solid, m.p. 267-268°C. ^{1}H NMR (400 MHz, $CDCl_3$) δ (ppm): 10.03 (s, 2H,), 8.51 (d, 2H, *J* = 9.2 Hz), 8.26 (d, 2 H, *J* = 8.0 Hz), 8.16 (m, 4 H), 7.94 (d, 2H, *J* = 3.8 Hz) 7.51 (d, 2H, *J* = 3,8 Hz), ^{13}C NMR (100 MHz, $CDCl_3$) δ (ppm): 183.63, 136.84, 136.50, 131.50, 129.51, 129.20, 128.79, 128.68, 128.57, 125.47, 125.38, 125.21; HRMS (APCI+) calc. For $C_{26}H_{14}O_2S_2$ $[M+H]^+$: 423.0513; found: 423.0528.

*General procedure for synthesis of **1-4***

Aldehydes or dialdehydes **5, 6, 7** and **9** (1 mmol) and a few drops of Et_3N were dissolved under stirring in 30 mL $CHCl_3$ and hexylcyanoacetate (4 mmol for **5** and **7** and 8 mmol for **6** and **9**) was added dropwise. The reaction mixture was refluxed under stirring for 24 h. After return to r.t. the solvent was removed in vacuum and the product was chromatographed on silica gel.

Hexyl-2-cyano-3-[4'-(pyren-1''-yl)benzen-1'-yl]acrylate (**1**).

Eluent 20:3 PE/AcOEt. Yield 110 mg (43 %). Yellow solid, m.p. 114-115 °C. ^{1}H RMN (400 MHz, $CDCl_3$) δ (ppm): 8.38 (s, 1H), 8.26-8.02 (overlapped peaks, 10H), 7.98 (d, *J*=7.8 Hz, 1H), 7.81 (d, *J*=8.1 Hz, 2H), 4.36 (t, *J*=6.7 Hz, 2H), 1.80 (m, 2H), 1.54-1.34 (overlapped peaks, 6H), 0.93 (t, *J*=7.5 Hz, 3H). ^{13}C RMN (100 MHz, $CDCl_3$) δ (ppm):162.86, 154.71, 146.77, 131.64, 131.58, 131.40, 131.36, 131.02, 130.53, 128.49 128.29, 128.15, 127.48, 127.43, 126.38, 125.69, 125.37, 125.13, 124.92, 124.71, 115.84, 102.96, 67.06, .31.54, 28.64, 25.63, 22.67, 14.15. HRMS (APCI+) calcd. for $C_{32}H_{28}NO_2$ $[M+H]^+$: 458.2115; found: 458.2104.

Dihexyl-3,3'-[4,4'-(pyrene-1,6-diyl)bis(benzene-1,4-diyl)]bis(2-cyanoacrylate) (**2**).

Eluent 3:5 DCM/PE. Yield 185 mg (71 %). Yellow solid, m.p. 189-190°C. ^{1}H RMN (400 MHz, $CDCl_3$) δ (ppm): 8.39 (s, 2H), 8.26 (d, 2H, *J* = 7.9 Hz), 8.21 (d, 4H, *J* = 8.3 Hz), 8.20 (d, 2H, *J* = 9.2 Hz), 8.10 (d, 2H, *J* = 9.2 Hz), 8.02 (d, 2H, *J* = 7.8 Hz), 7.81 (d, 4H, *J* = 8.3 Hz), 4.37 (t, 4H, *J* = 6.7 Hz), 1.80 (m, 4H), 1.48-1.43 (overlapped peaks, 4H), 1.39-1.34 (overlapped peaks,

8H), 0.93 (t, 6H, *J* = 6.9 Hz). ^{13}C RMN (100 MHz, $CDCl_3$) δ (ppm):162.84, 154.66, 146.64, 131.68, 131.39, 131.12, 130.66, 128.84, 128.21, 127.83, 125.33, 125.30, 125.17, 115.82, 103.12, 67.09, 31.54, 28.65, 25.64, 22.68, 14.16. HRMS (APCI+) calcd. for $C_{48}H_{45}N_2O_4$ $[M+H]^+$: 713,3374; found: 713.3351.

Hexyl-2-cyano-3-[(5'-pyren-1''-yl)thiophene-2'-yl]acrylate (**3**).

Eluent 3:1 PE/AcOEt, Yield 70mg (38%). Orange solid, m.p. 139-140 °C. ^{1}H NMR (600 MHz, $CDCl_3$) δ (ppm): 8.46 (d, 1H, , J = 9.2 Hz), 8.41 (s, 1H), 8.24 (overlapped peaks, 4 H), 8.15 (overlapped peaks, 1H), 8.12 (t, 1H, *J* = 8.2 Hz), 8.07 (t, 1H, *J* = 7.6 Hz), 7.95 (d, 1H, *J* = 3.8 Hz), 7.53 (d, 1H, J = 3.8 Hz), 4.33 (t, 2H, *J* = 6.7 Hz), 1.78 (m, 2H), 1.44 (overlapped peaks, 2H) 1,35 (overlapped peaks, 2H), 1.25 (overlapped peaks, 2H), 0.92 (t, 3H, J =7.0 Hz). ^{13}C NMR (150 MHz, $CDCl_3$) δ (ppm): 163.19, 153.58, 146.65; 138.18; 136.56; 132.19; 131.54; 130.93; 129.58; 129.03; 128.99, 128.77; 128.33; 127.90; 127.44; 126.60; 126.12; 125.75; 125.18; 124.89; 124.75; 124.27; 116.13; 98.72; 66.82; 31.54, 28.68, 25.64, 22.67, 14.15. HRMS (APCI+) calcd. for $C_{30}H_{25}NO_3S$ $[M+H]^+$: 464.1732; found: 464.1749.

Dihexyl-3,3'-[5,5'-(pyrene-1,6-diyl)bis(thiophene-5,2-diyl)]bis(2-cyanoacrylate) (**4**).

Eluent 5:2 DCM/PE. Yield 520 mg (43%).Yellow-orange solid, m.p. 245-246°C. ^{1}H NMR (400 MHz, $CDCl_3$) δ (ppm): 8.51 (d, 2H, *J* = 9.2 Hz), 8.41 (s, 1H), 8.24 (s, 1H), 8.25 (d, 2H, *J* = 8.0 Hz), 8.17 (dd, 4H, *J* = 3.2 Hz, 8.0 Hz), 7.96 (d, 2H, *J* = 3.9 Hz), 7.53 (d, 2H, *J* = 3.9 Hz), 4.16 (t, 4H, *J* = 6.7 Hz), 1.79 (m, 4H), 1.44 (overlapped peaks, 4H); 1.35 (overlapped peaks, 8H), 0.92 (t, 6H, *J* =6.9 Hz)^{13}C NMR (150 MHz, $CDCl_3$) δ (ppm): 163.12; 155.16; 146.63; 138.23; 136.81; 131.71; 129.80; 129.33; 128.91; 128.88; 128.82; 125.48; 125.46; 125.15; 116.09; 98.97; 66.87; 31.54; 28.66; 25.63; 22.67; 14.16. HRMS (APCI+) calcd. for $C_{44}H_{40}N_2O_4S_2$ $[M+H]^+$: 725.2502; found: 725.2525.

Acknowledgements

This work was financially supported by the project SMOSCs, ID: 37_220, Cod MySMIS: 103509 funded by the Romanian Ministry for European Funds through the National Authority for Scientific Research and Innovation (ANCSI) and co-funded by the European Regional Development Fund / Competitiveness Operational Program 2014-2020 (POC) Priority Axis 1 / Action 1.1.4

References

[1]. Figueira-Duarte TM, Müllen K. Pyrene-Based Materials for Organic Electronics, Chem Rev 2011; 111: 7260-7314.

[2]. Carati C, Gasparini N, Righi S, Tinti F, Fattori V, Savoini A, Cominetti A, Po R, Bonoldi L, Camaioni N, Pyrene-Fullerene Interaction and Its Effect on the Behavior of Photovoltaic Blends, J Phys Chem C 2016; 120: 6909-6919.

[3]. Cominetti A, Pellegrino A, Longo L, Po R, Tacca A, Carbonera C, Salvalaggio M, Baldrighi M, Valdo Meille S, Polymer solar cells based on poly(3-hexylthiophene) and fullerene:Pyrene acceptor system, Mater Chem Phys 2015; 159 : 46-55.

[4]. Chen RJ, Zhang Y, Wang D, Dai H, Noncovalent Sidewall Functionalization of Single-Walled Carbon Nanotubes for Protein Immobilization, J Am Chem Soc 2001; 123: 3838-3839.

[5]. Yassin A, Jimenez P, Lestriez B, Moreau P, Leriche P, Roncali J, Blanchard P, Terrisse H, Guyomard, Gaubicher J, Engineered Electronic Contacts for Composite Electrodes in Li Batteries Using Thiophene-Based Molecular Junctions, Chem Mater 2015; 77: 4057-4066.

[6]. Lee D-W, Kim T, Lee M, An amphiphilic pyrene sheet for selective functionalization of graphene, Chem Commun 2011; 47**:** 8259-8261.

[7]. Moggia F, Videlot-Ackermann C, Ackermann J, Raynal P, Brisset H, Fages F, Synthesis and thin film electronic properties of two pyrene-substituted oligothiophene derivatives, J Mater Chem 2006; 16: 2380-2386.

[8]. Tao J, Liu D, Qin Z, Shao B, Jing J, Li H, Dong H, Xu B, Tian W, Organic UV-Sensitive Phototransistors Based on Bistriphenylamineethynylpyrene Derivatives with Ultra-High Detectivity Approaching 10^{18}, Adv Mater 2020;1907791.

[9]. Kwon J, Hong J-P, Noh S, Kim T-M, Kim J-J, Lee C, Lee S, Hong J-Y, Pyrene end-capped oligothiophene derivatives for organic thin-film transistors and organic solar cells, New J Chem 2012; 36: 1813-1818.

[10]. Zhu X-H, Peng J, Cao Y, Roncali J, Solution-processable single-material molecular emitters for organic light-emitting devices, Chem Soc Rev 2011; 40: 3509-3524.

[11]. Feng X, Hu J-Y, Redshaw C, Yamato T, Functionalization of Pyrene To Prepare Luminescent Materials-Typical Examples of Synthetic Methodology, Chem Eur J 2016; 22: 11898-11916.

[12]. Moorthy JN, Natarajan P, Venkatakrishnan P, Huang D-F, Chow TJ, Steric Inhibition of π-Stacking: 1,3,6,8-Tetraarylpyrenes as Efficient Blue Emitters in Organic Light Emitting Diodes (OLEDs), Org Lett 2007; 25: 5215 -5218.

[13]. Thomas KRJ, Kapoor N, Bolisetty MNKP, Jou J-H, Chen Y-L, Jou Y-C. Pyrene-Fluorene Hybrids Containing Acetylene Linkage as Color Tunable Emitting Materials for Organic Light-Emitting Diodes, J Org Chem 2012; 77: 3921-3932.

[14]. Yu C-C, Jiang K-J, Huang J-H, Zhang F, Bao X, Wang F-W, Yang L-M, Song Y. Novel pyrene-based donor–acceptor organic dyes for solar cell application. Org Electron 2013; 14: 445-450.

[15]. Lee OP, Yiu AT, Beaujuge PM, Woo CH, Holcombe TW, Millstone JE, Douglas JD, Chen MS, Fréchet JMJ, Efficient Small Molecule Bulk Heterojunction Solar Cells with High Fill Factors via Pyrene-Directed Molecular Self-Assembly, Adv Mater 2011; 23: 5359-5363.

[16]. Lee S-Y, Jung CH, Kang J, Kim H-J, Shin WS, Yoon SC, Moon SJ, Lee C, Hwang DH, Synthesis of a New Conjugated Polymer Composed of Pyrene and Bithiophene Units for Organic Solar Cells, Nanosci Nanotechnol 2011; 11: 4367-4372.

[17]. Kim J-H, Lee S, Kang I-N, Park M-J, Hwang D-H. Photovoltaic devices using semiconducting polymers containing head-to-tail-structured bithiophene, pyrene, and benzothiadiazole derivatives, J. Polym. Sci. A. Polym. Chem. 2012; 50: 3415-3424.

[18]. Jousselin-Oba T, Sbargoud K, Vaccaro G, Meinardi F, Yassar A, Frigoli M. Novel Fluorophores based on Regioselective Intramolecular Friedel–Crafts Acylation of the Pyrene Ring Using Triflic Acid, Chem Eur J 2017; 23: 16184-16188.

[19]. Wang Y, Liu B, Koh CW, Zhou X, Sun H, Yu J, Yang K, Wang H, Liao Q, Woo HY, Guo X, Facile Synthesis of Polycyclic Aromatic Hydrocarbon (PAH)–Based Acceptors with Fine-Tuned Optoelectronic Properties: Toward Efficient Additive-Free Non-fullerene Organic Solar Cells, Adv Energy Mater 2019;1803976.

[20]. Liu M, Gong X, Zheng C, Gao D. Development of Pyrene Derivatives as Promising n-Type Semiconductors: Synthesis, Structural and Spectral Properties. Asian J Org Chem 2017; 6: 1903-1913.

[21]. Roncali J, single-material organic solar cells: the next frontier for organic photovoltaics. Adv Energy Mater 2011; 1: 147-160.

[22]. Roncali J, Grosu I, The dawn of single-material organic solar cells, Adv Sci 2019; 6:1801026.

[23]. Diac A, Szolga L, Cabanetos C, Bogdan A, Terec A, Grosu I, Roncali J. C_{60}-small arylamine push-pull dyads for single-material organic solar cells. Dyes & Pigments 2019; 171: 107748.

[24]. Zhang G, Zhao J, Chow PCY, Jiang K, Zhang J, Zhu Z, Zhang J, Huang F, Yan H. Nonfullerene Acceptor Molecules for Bulk Heterojunction Organic Solar Cells. Chem Rev 2018; 118: 3447-3507.

[25]. Chatterjee S, Ghosh S, Mishra S, Das Saha K, Banerji B, Chattopadhyay K, Efficient Detection of Early Events of α-Synuclein Aggregation Using a Cysteine Specific Hybrid Scaffold Biochemistry, 2019 ; 58 :1109-1119.

[26]. Baheti A, Lee C-P, Thomas J, Ho K-C, Pyrene-based organic dyes with thiophene containing π-linkers for dye-sensitized solar cells: optical, electrochemical and theoretical investigations, Phys Chem Chem Phys, 2011; 13: 17210-17221.

[27]. Li, Y.; Chen, Q.; Xu, T.; Xie, Z.; Liu, J.; Yu, X.; Ma, S.; Qin, T.; Chen, L., De Novo Design and Facile Synthesis of 2D Covalent Organic Frameworks: A Two-in-One Strategy, J Am Chem Soc, 2019; 141: 13822-13828.

[28]. Idzik KR, Licha T, Lukes V, Rapta P, Fryfel J, Schaffer M, Taeuscher E, Beckert R, Dunsch L, Synthesis and Optical Properties of Various Thienyl Derivatives of Pyrene. J. Fluoresc. 2014 ; 24: 153-160.

[29]. Kathiravan, A.; Srinivasan, V.; Khamrang, T.; Velusamy, M.; Jaccob, M.; Pavithra, N.; Anandan, S.; Velappan, K. Pyrene Based D-π-A Architectures: Synthesis, Density Functional Theory, Photophysics and Electron Transfer Dynamics. Phys Chem Chem Phys, 2017; 19: 3125-3135.

[30]. Ashizawa M, Yamada K, Fukaya A, Kato R, Hara K, Takeya J, Effect of Molecular Packing on Field-Effect Performance of Single Crystals of Thienyl Substituted Pyrenes, Chem Mater, 2008 ; 20 : 4883-4890.

[31]. Roquet S, Cravino A, Leriche P, Alévêque O, Frère P, Roncali J. Triphenylamine-thienylenevinylenes Hybrid Systems with Internal Charge-transfer as Donor Materials for Hetero-junction Solar Cells, J Am Chem Soc 2006; 128: 3459-346.

[32]. Roncali J, Synthetic Principles for Bandgap Control in Linearly pi-Conjugated Systems, Chem Rev 1997; 97: 173-205.

[33]. Barbarella G, Zambianchi M, Bongini A, Antolini L, The deformability of the thiophene ring: A key to the understanding of the conformational properties of oligo- and polythiophenes, Adv Mater 1993; 5: 834-838.